THE INTERACTION BETWEEN SECONDARY FLOW AND FILM COOLING IN A TURBINE NOZZLE

by
C. Langowsky
Research Engineer, Institute for Propulsion Technology
German Aerospace Research Establishment
DLR, Linder Höhe, D-51147 Cologne

Abstract

An annular film cooled turbine nozzle with cooling air ejection on the stator leading edge and the suction side is experimentally investigated concerning the interaction between the cooling air and the secondary flow at local Blowing ratios of $0 \le M_l \le 1.4$. The influence of the radial pressure gradient on film cooling, the development of the cooling air jets and the mixing process are studied to explain the different loss production with varied Blowing ratios, mainly on the tip. The flow field downstream of the nozzle is measured using a 5-hole probe to quantify the loss production. Furthermore, Laser-Light-Sheet and oilflow experiments are carried out to visualize the interaction of the two fluid streams. The cooling air jets are dragged along by the secondary flow and show a different mixing behaviour, depending on the Blowing ratio. Thus, non cooled respectively badly cooled areas can be indicated and an insight into the origin of the loss production is possible. A detailed analysis is presented in this paper.

Nomenclature

C	[m]	chord length
d	[m]	diameter
h	[m]	blade height
$\dot{m}$	[kg/s]	mass flow rate
M		Blowing ratio, $M = \frac{(\rho v)_c}{(\rho v)_0}$
Ma		Mach number
p	[bar]	pressure
r	[m]	radius
Re		Reynolds number, $Re = \frac{\overline{v}_1 \cdot C_{MS}}{\nu}$
s	[m]	pitch of cooling holes
T	[K]	temperature
Tu	[%]	turbulence level
v	[m/s]	velocity
x,y,z		cartesian coordinates
α	[°]	circumferential flow angle
β	[°]	radial flow angle
ζ		kinetic energy loss coefficient
ν	[m/s^2]	kinematic viscosity

Subscripts and Superscripts

0	upstream condition
1	downstream condition
ax	axial direction
c	cooling air
ex	cooling hole exit
H	hub
l	local
m	mainflow region
MS	mid-span
rel	relative
s	secondary flow region
st	static condition
t	total condition
T	tip
—	averaged

Symbols

MP	measuring plane
SS	suction side
TE	trailing edge

Introduction

The permanent increase of power demand and air traffic requires economical gas turbine engines with a high performance. This need can be reached among other things with an increased turbine inlet temperature. But even newly developed high temperature resistant blade materials are not able to meet the thermal requirements. Film cooling in addition to a sophisticated interior cooling system is a very effective method of protecting the nozzle blades from the hot gas environment.

During the introduction of film cooling the thermal efficiency was the main topic of research work. Thereby numerous scientific investigations are concentrated on the heat transfer characteristics of the film cooling process [4,9,12,14]. Because economy can only be obtained by the symbiosis of thermal and aerodynamic optimum the aerodynamic consequences of cooling air ejection to the stator main flow and the loss behaviour became more interesting. Most of the previous studies [5,13,27,28] present the change of the loss coefficient with film cooling, but does not give an explanation of the mechanisms by which the losses are produced. Individual effects like the the secondary flow development [19,24,26] or the mixing behaviour of jets in crossflow [1,21,25] are studied in detail, but there is not an extensive knowledge about the complexity of its interaction.

This study is a comprehensive experimental investigation of a film cooled annular turbine cascade with regard to the influence of cooling air ejection on the whole stator aerodynamics.

Here of importance is the interaction between the strong endwall secondary flow and the ejected cooling air with varied Blowing ratios. It is the first attempt to explain the complex interaction of the above mentioned effects and their contribution to the stator loss production.
Therefore, the losses are quantified by 5-hole probe measurements downstream of the nozzle. Oil flow experiments indicate the disturbance of the secondary flow development by the ejected air. The visualisation of the ejection process by Laser-Light-Sheet experiments show the radial distribution of the ejected cooling air. Due to the quantitative imaging technique information about the cooling air concentration is available and conclusions on the mixing process can be made.

Test facility

The experiments were carried out at the DLR annular turbine cascade with 25 blades. The tested stator is a scaled version (scaling factor 2.348) of a subsonic, low aspect ratio turbine nozzle with constant hub and tip radii. The cascade is an open loop continuously operating facility with cold air (maximum temperature 315 K, maximum pressure 2.0 bar) and the following main dimensions:

hub diameter, d_H	0.315 m
tip diameter, d_T	0.400 m

The cascade includes four film cooled blades enclosing the test passage in the middle. Cooling air is supplied from a separate pressure vessel up to a maximum temperature of 310 K. The experiments were carried out at equal temperatures of cooling air and main flow. Test results of [3,23] showed that the density ratio had a significant influence on the film cooling effectiveness, but [6,8] found a negligible effect of $\leq 1\%$ on the stator loss production. Thus, the influence of the density ratio existing in a real turbine need not be considered for the analysis of the stator aerodynamics. The flow field downstream of the blade row was measured using a 5-hole probe with 17 radial and 18 circumferential measuring positions. The main dimensions of the blade geometry are indicated as follows:

pitch angle	14.4°
chord length at mid span, C_{MS}	0.0698 m
aspect ratio, h/C	0.61
inlet flow angle, α_0 (circumf.)	90°
inlet flow angle, β_0 (radial)	0°
outlet flow angle, α_1	20°

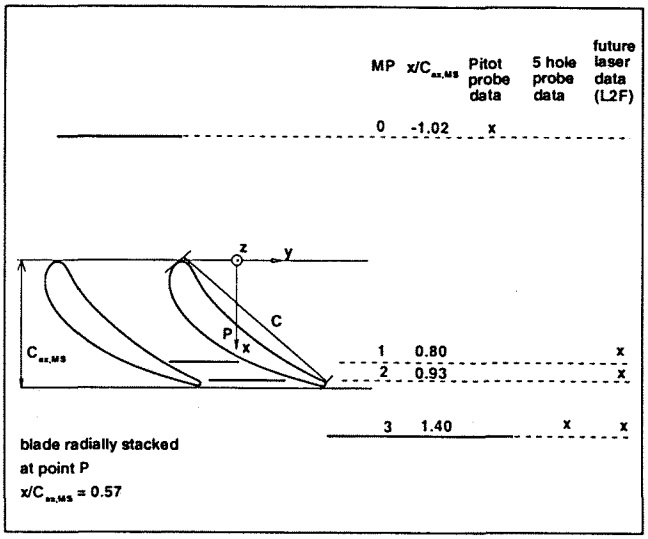

Fig.1:Cascade geometry at mid-span and measurement plane

Fig.1 shows the axial position of the measuring planes and Fig.2 the arrangement of the rows for cooling air ejection including the geometric data of the axial row position as well as the characteristics of the hole geometry.

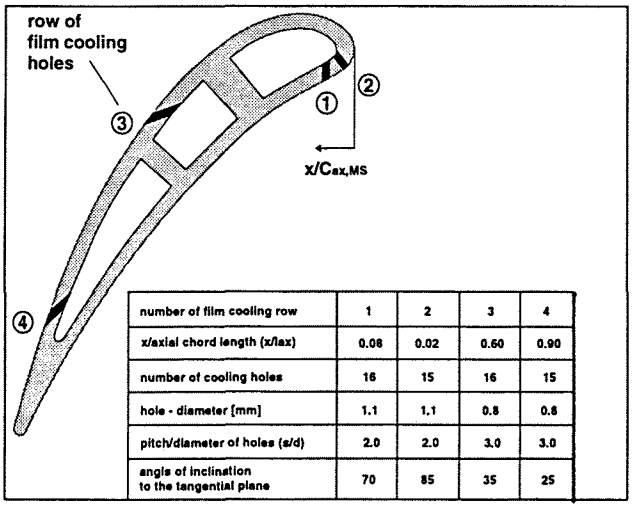

number of film cooling row	1	2	3	4
x/axial chord length (x/lax)	0.08	0.02	0.60	0.90
number of cooling holes	16	15	16	15
hole - diameter [mm]	1.1	1.1	0.8	0.8
pitch/diameter of holes (s/d)	2.0	2.0	3.0	3.0
angle of inclination to the tangential plane	70	85	35	25

Fig. 2: Arrangement of film cooling rows

The operating point at which the measurements were carried out is quantified below:

mass flow rate, m_0	5.315 kg/s
total inlet pressure, p_{t0}	1.6220 bar
total inlet temperature, T_{t0}	305.0 K
turbulence level, Tu_0	4.4 %
inlet Mach number, Ma_0	0.1745
outlet Mach number, Ma_1	0.74
Reynolds number, Re_1	1×10^6
coolant temperature, T_{tc}	305.0 K
local Blowing ratio, $M_1 = \frac{(\rho v)_c}{(\rho v)_0}$	0.5/1.0/1.4

The measurement of the incoming boundary layers show that they are turbulent both on hub and tip and have a thickness of about 4.5% blade height. The results of 5-hole probe measurements upstream shows that the inlet flow angle is uniform.

Measurement techniques

5-hole-probe

The measured variables of the 5-hole probe are evaluated three dimensionally. For this application the probe has to be calibrated for the two flow directions α, β and Mach number. Polynomial approximations are used to relate the data of calibration with the measurement data. The accuracy of the 5-hole probe data is as followed:

- flow angles α, β $\pm 0,5^\circ$
- total pressure, p_t $\pm 0,1$ mbar

The probe is fixed at the average outlet flow angle $\bar{\alpha}_1$. It has to move only in the radial direction. Pitchwise traversing was achieved by turning the complete stator hub with the blades. The resultant tip leakage is prevented by a tiny plastic seal.

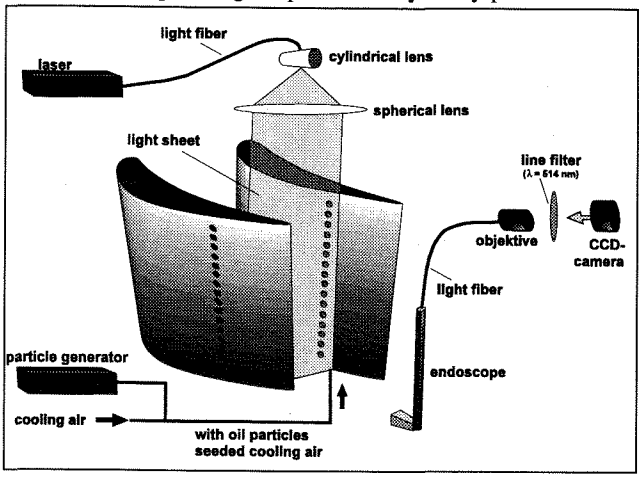

Fig. 3: Schematic sketch of radial Laser-Light-Sheet

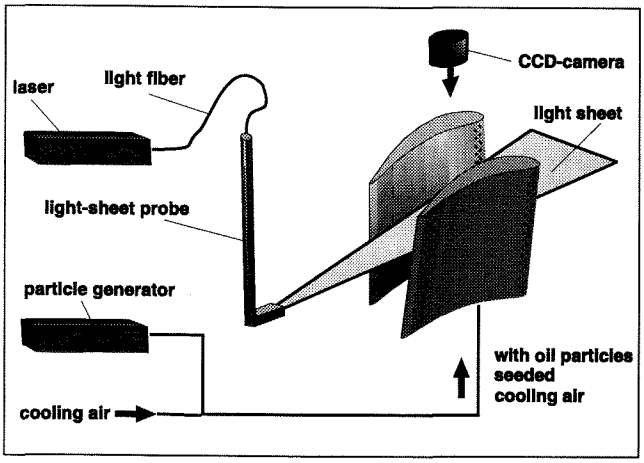

Fig. 4: Schematic sketch of axial Laser-Light-Sheet

Laser-Light-Sheet

The aim of the quantitative Laser-Light-Sheet imaging technique is to quantify concentrations in mixing flows. The underlying Lorenz-Mie theory claims that the elastically scattered light is proportional to the number of particles in the probe volume and hence proportional to the concentration of the cooling air, which is seeded with small particles of vapourized propanediol oil injected into the flow. The light source is an argon ion laser with an average power of 3.5 W, working in multiline mode.

The radially spread Light-Sheet is created outside the cascade by the succession of a cylindrical and a spherical lens in the path of the laser beam (see Fig.3). The ejection process is recorded using a CCD-camera. By means of an endoscope observation against the flow direction is allowed without affecting the flow field . But the optics need to be protected and this is achieved by blowing out air from a surrounding duct to prevent pollution of the front lens by hitting of particles.

The axially spread Light-Sheet, Fig.4, is created inside the cascade by a Laser-Light-Sheet probe. Because it is also directed against the mainflow the protection of the optics is required again obtained by the same principle as described above. For this test setup the CCD-camera is installed outside.

The camera signals are digitized and subsequently pseudo-colored for a better evaluation of the concentration. Details about the image processing and the installation of the laser and the optics are described in [15].

Oil-flow

For the oil flow experiments a mixture of titanium dioxide and oil of appropriate viscosity is applied to the blade surface. Lower shear stresses (e. g. laminar boundary layers or areas of separation) can be identified by white-looking areas, because more particles remain on the surface. Dark parts identify the higher shear stresses of turbulent boundary layers.

Results and discussion

The secondary flow in a turbine passage is a complex system of different vortices. The passage vortex is the largest one. Its extension depends on the incoming boundary layer thickness rolling up to the horse-shoe vortex in front of the leading edge at both endwalls. After rolling up, the vortex splits into two parts. Due to the pressure gradient in the blade to blade direction, the pressure side leg drifts through the passage to the suction side absorbing boundary layer material of the endwall. This fusion is called the passage vortex, which affects a triangular area on the suction side. This area is smaller on the hub since the radial pressure gradient forces this vortex to the hub. The streamline pattern on the suction side with the drifting boundary layer material is shown in Fig.12.

Cooling air ejection in the region affected by the secondary flow disturbs its development and affects simultaneously the production of the aerodynamic losses depending on the Blowing ratio. Typically the losses of turbomachine components are described by loss coefficients. With the commonly used pressure loss coefficient the energy transformation of a film cooled nozzle can be judged only insufficiently, since the energy of the added cooling air is not considered. This influence can be taken into account by the kinetic energy loss coefficient ζ_{kin} as follows, for n film cooling rows:

$$\zeta_{kin} = 1 - \frac{\left(1-\left(\frac{\overline{p_{st1}}}{\overline{p_{t1}}}\right)^{\frac{\kappa-1}{\kappa}}\right)\cdot\left(1+\frac{(\dot{m}\cdot c_p\cdot T_t)_c}{(\dot{m}\cdot c_p\cdot T_t)_0}\right)}{\left(1-\left(\frac{\overline{p_{st1}}}{\overline{p_{t0}}}\right)^{\frac{\kappa-1}{\kappa}}\right)+\sum_{i=1}^{n}\frac{(\dot{m}\cdot c_p\cdot T_t)_{c,i}}{(\dot{m}\cdot c_p\cdot T_t)_0}\cdot\left(1-\left(\frac{\overline{p_{st,1}}}{\overline{p_{tc,ex,i}}}\right)^{\frac{\kappa-1}{\kappa}}\right)}$$

The averaged values are determined as below:

$\overline{p_t}$ mass averaged

$\overline{p_{st}}$ area averaged

In this analysis the losses arising in the cooling holes are neglected. Fig.5 presents the kinetic loss production ζ_{kin} for different Blowing ratios. Since the two fluid streams have an

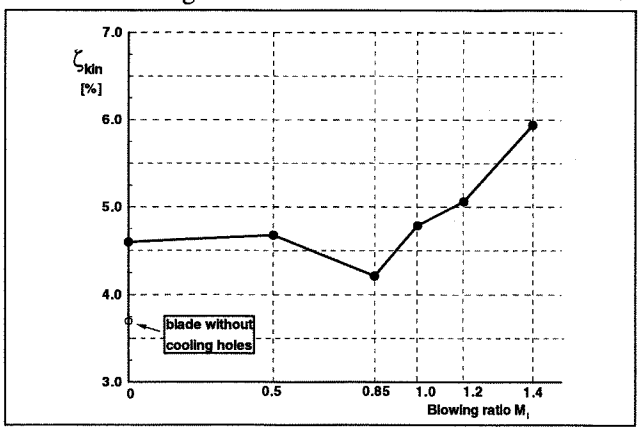

Fig. 5: Total loss of kinetic energy for row 4 and different Blowing ratios

identical total temperature and constant-pressure mixing is presumed, the density difference is negligibly small and the Blowing ratio represents under these assumptions the velocity ratio. Thus, for $M_I < 1$ low momentum ejection exists and for $M_I > 1$ high momentum ejection.

The influence of alone the existence of the blowing holes is demonstrated for the uncooled blade (M_I=0). They induce an earlier transition from laminar to turbulent boundary layer. This results in a loss increase of about 1% in comparison to the smooth blade. Increasing cooling air ejection a minimum loss production occurs for M_I=0.85. Because the boundary layer has a momentum deficit, the lowest shearing stresses arise for ejection with a slightly smaller momentum than the mainstream. Consequently there is an almost loss free mixing of the coolant. For $0 < M_I < \sim 0.5$, ζ_{kin} is insignificantly higher compared to zero ejection. The losses rise rapidly for $M_I > 0.85$ because of the the increase in fluid interaction. The same trend in loss production is confirmed by the investigations of Wilfert [25].

To find the origin of the varying loss behaviour the radial distribution of ζ_{kin} (Fig.6) is analyzed indicating clear tendencies. Shown are the loss distributions for typical Blowing ratios M_I =0/0.5/0.86/1.4 with different characters of momentum ratios. The loss maximum on the hub caused by the secondary flow and its interaction with the cooling air does not change its location and is nearly of the same order of magnitude. The above described mixing loss behaviour is clearly visible in the region around the mid-span where no secondary flow is present. Significant differences exist on the tip. While the low momentum ejection (M_I=0.5) shows an apparent profit of kinetic energy of about 1.7%, the loss of energy increases for the high momentum ejection (M_I=1.4) by about 2.9% relatively to non cooling. There are four different influences which explain this effect:

- the radial distribution of ejected cooling air due to the radial pressure gradient
- the different mixing behaviour of ejected cooling air in the region influenced by the secondary flow versus the mainflow region dependent on the Blowing ratio
- different penetration of cooling air jets into the mainflow
- the different orientation of cooling air jets with respect to the secondary flow direction dependent on the Blowing ratio

In the following the influence of each point on the kinetic energy loss production is discussed separately.

Fig.7 presents the variation of the radial cooling air distribution with the radial pressure gradient represented by the static pressure ratio $p_{st,T}/p_{st,H}$ at the position of ejection and the Blowing ratio. The strongest difference of the ejected cooling air massflow at the hub and at the tip exists for small Blowing ratios. Raising the Blowing ratio by increasing the total pressure of the cooling air $p_{t,c}$ this variation is reduced and nearly disappears for $M_I > 1$. A recalculated radial distribution of the kinetic energy loss for M_I=0.5 taking into accout the real radial distribution of ejected cooling air does not change the local losses evidently. Although there is a remarkable difference of ejected cooling air between hub and tip of about 33%, the total coolant massflow is only ~0.8% of the mainflow and therefore has a weak influence

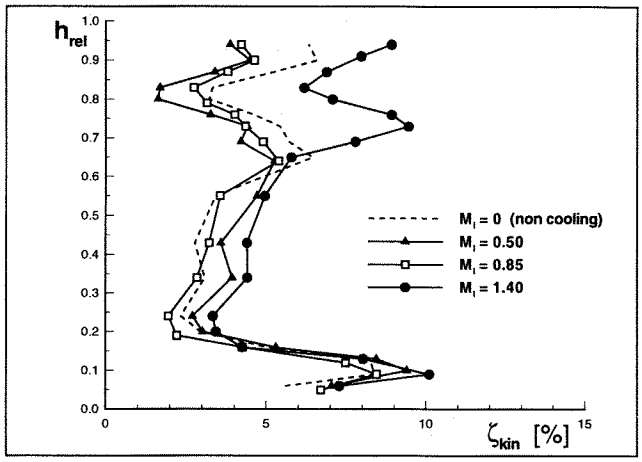

Fig. 6: Radial distribution of the kinetic energy loss

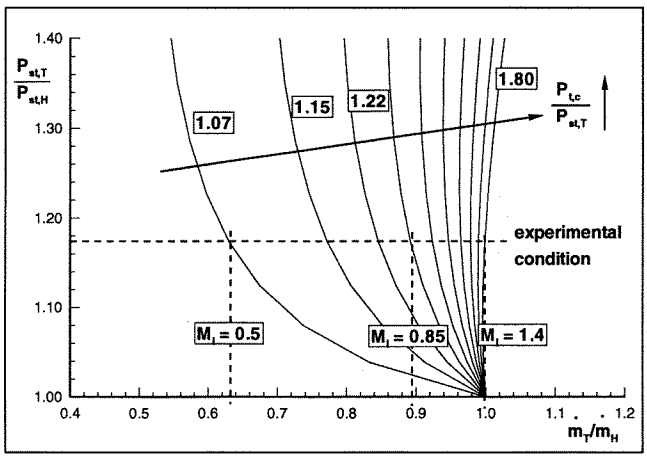

Fig. 7: Variation of radial cooling air distribution

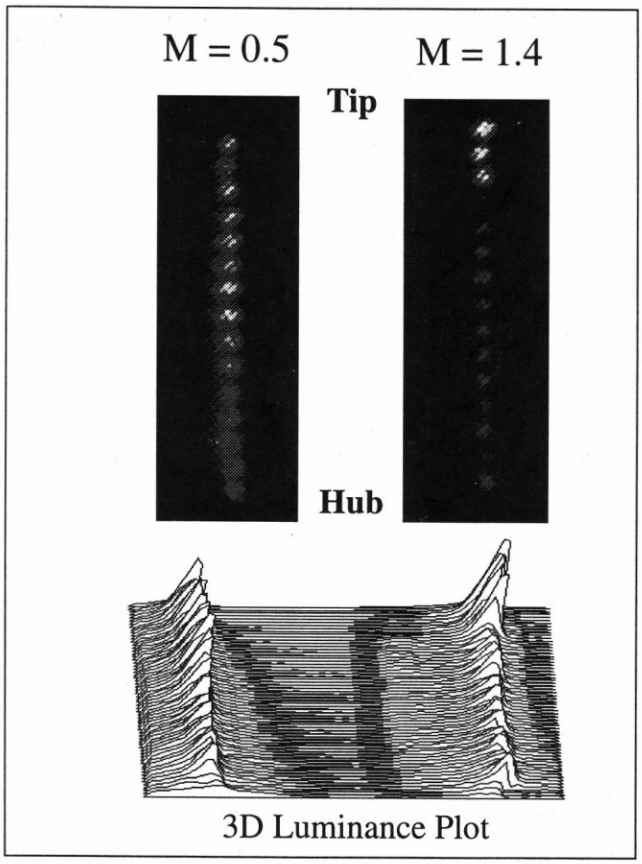

Fig. 8: Radial distribution of coolant concentration (row 4)

on the loss production. But for surface cooling this fact should be paid attention to because less cooling air is available on the tip for smaller Blowing ratios.

The radial Laser-Light-Sheet experiments expose an interesting behaviour of the cooling air mixing process. A connection between the secondary flow region, the Blowing ratio and the cooling air concentration can be identified. Fig.8 demonstrates the radial distribution of the cooling air concentration for M_l=0.5 and M_l=1.4 immediately downstream of film cooling row 4. In the figure the luminance is connected with the number of light reflecting oil particles and thus proportional to the cooling air concentration.

Clearly visible is the intensified cooling air concentration of the first *three* jets at the tip only for M_l=1.4. Oil flow experiments prove that they are located in the region which is affected by the secondary flow (see also Fig. 12). At this point the question arises as to why such a difference in the cooling air concentration between the secondary flow and mainstream region only exists for M_l=1.4 although for M_l=0.5 the same jets are influenced by the secondary flow?

Two fundamental differences exist between the secondary flow domain and the unaffected mainflow region. Because the passage vortex consists of accumulated boundary layer material, it is, firstly, of lower velocity and, secondly, of higher turbulence level. Numerical flow calculations with modelled cooling air ejection demonstrate the correct simulation of the secondary flow and the film cooling [16] and quantify this fact to a velocity reduction to 88% of the mainflow value with a 6% higher turbulence level.

Basis for the definition of the blowing ratio is only the axial component of the velocity. The above mentioned facts lead to a different ejection behaviour in the secondary flow region corresponding to the blowing ratio, as following described.

M_l=0.5

Two effects exist, which influence the cooling air concentration in the secondary flow region.

The first operates intensifying the concentration. The oilflow pattern for M_l=0.5 in Fig.12 indicate that the cooling air of low energy is deflected on the blade tip by the secondary flow and shows the same flow direction of around 35° deflection against the mainflow. The flow situation in the region of interest is sketched in Fig. 9.

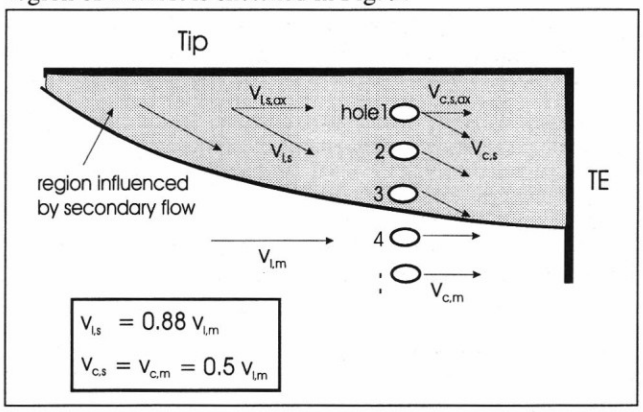

Fig. 9: Schematic sketch of velocity ratios for M_l=0.5

The behaviour of the neighbouring jets 3 and 4 are analyzed assuming constant densities and cooling air velocities. This results in a 14% higher Blowing ratio respectively mass flow density in the region of the secondary flow. Thus, the cooling air concentration should be higher there.

The second effect operates diminishing the concentration. Investigations of [10,11] found a significant effect of the mainstream turbulence level on the jet propagation. The jets are soon mixed with the mainflow for a large main-stream turbulence level, but well preserved for smaller levels. Measurements of [2,20] show a decreasing film cooling effectiveness with increasing turbulence levels for low Blowing ratios due to the faster mixing process.

For M_l=0.5 it seems that both effects compensate each other because no clearly difference in the cooling air concentration can be observed in Fig. 8.

M_l=1.4

Different conditions are present for M_l=1.4. The oilflow pattern of Fig.13 shows an almost axial propagation for the higher energized cooling air jets, also in the secondary flow region. As described above, the local Blowing ratio is evaluated with the axial component of the velocity. Furthermore, the same presumptions as for M_l=0.5 are valid. The actual conditions of the velocity ratios are demonstrated in Fig. 10. Thus, a nearly 40% higher mass flux density (local Blowing ratio) follows in the secondary flow region compa-

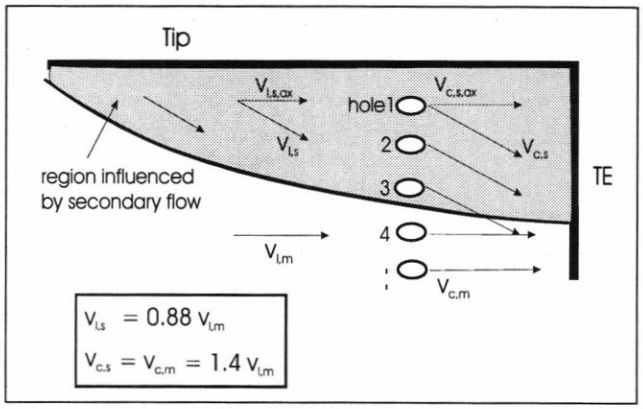

Fig. 10: Schematic sketch of velocity ratios for M_I=1.4

red to the mainflow. For high Blowing ratios the results of [2,20] show a negligible influence of the turbulence level on the film cooling effectiveness and corresponding to the mixing process, because the cooling air jets are more stable. Consequently, the increase of the mass flux density in the secondary flow region is three times higher than for M_I=0.5 and is the only effect present, which increases the concentration. This evident difference in the cooling air concentration for M_I=1.4 is clearly visible in Fig.8 and is also supported by the jet development pictures got from the axial Laser-Light-Sheet experiments. Fig.11 shows nearly uniform conditions of the cooling air concentration especially near the hole exit for M_I=0.5, meanwhile for M_I=1.4 an enormous increase in the region of secondary flow is visible.

The discharge coefficient of film cooling holes with their actual orientation does not have a strong influence on the ejected cooling air mass flow distribution. Extensive experiments of [7] prove a stronger effect of the crossflow condition on the discharge coefficient at the hole inlet (coolant side) than at the hole exit. The stronger the inlet crossflow the larger the reduction of the discharge coefficient. The crossflow at the hole exit has a much weaker influence but also tends to reduce its value.

The different penetration of the cooling air jets into the mainstream results in a different loss production. A deeper jet penetration for M_I=1.4 leads to stronger interactions with the mainstream and subsequently to a higher loss production. The different transport of the cooling air in the secondary flow region, already described above and also visible in the streamline patterns in Fig.12 and Fig.13 results in a different loss production. For M_I=1.4 the cooling air jets in the

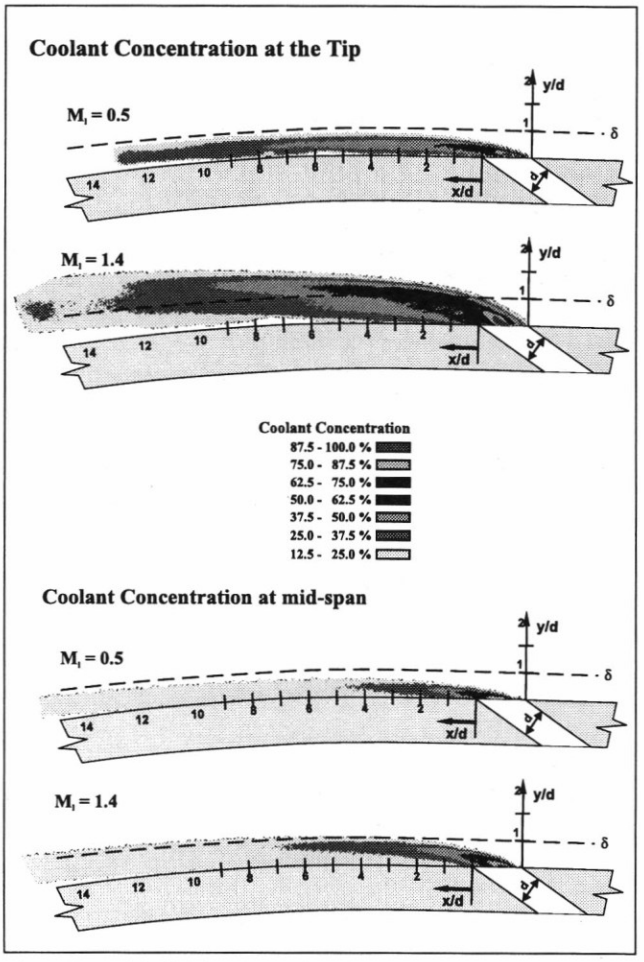

Fig. 11: Axial distribution of coolant concentration at the tip and at the mid-span

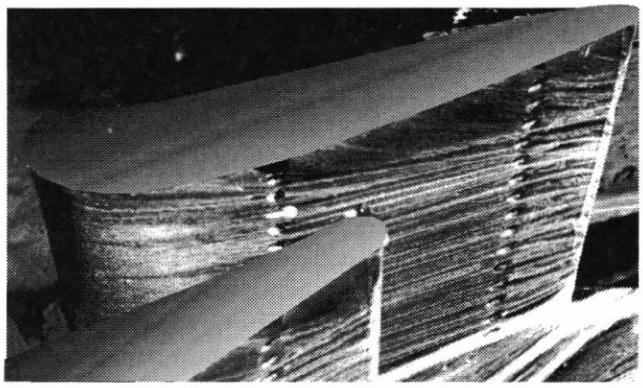

Fig. 12: Oilflow pattern for M_I = 0.5 (row4)

secondary flow region are ejected with an inclined angle of orientation (~ 40°) relative to the oncoming flow. A detailed analysis of [17] shows a better film coverage with increased orientation angles, but also a higher flow disturbance such as recirculation phenomena. Here the strength of flow disturbance strongly depends on the velocity ratio of the two fluid streams. The aerodynamic loss up to a velocity ratio of 1.0 is relatively small, regardless of the orientation angle. But the loss production drastically increases for the value of 2.0 (condition in the secondary flow region for M_I=1.4) already for small orientation angles. There is, for instance, an increase of the mixing losses of about 26% for the orientation angle of 45° compared to the parallel ejection. The largest aerodynamic loss is generated for an orientation angle of 90°. Thus, from the aerodynamic point of view the worst case is an additional deviation to the axial direction of cooling holes in the secondary flow region. A resultant orientation angle relative to the oncoming flow of around 90° with maximum loss production would follow. Experimental investigations of the film cooling effectiveness with compound angle holes [18,22] ,however, prove an increase of the

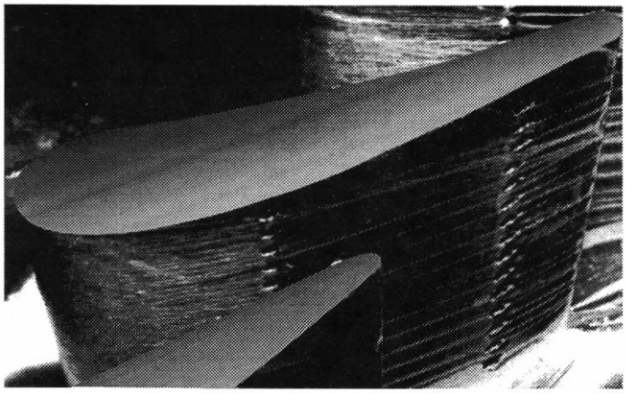

Fig. 13: Oilflow pattern for $M_1 = 1.4$ (row4)

film cooling effectiveness for increased orientation angles. Therefore a compromise between the aerodynamic and thermodynamic optimum has to be found. A first proposal which has to be studied in more detail is the cooling air ejection with the Blowing ratio of M_1=0.85. For this case the cooling air jets are energized enough to resist the deflection by the secondary flow in order to provide an effective cooling in the downstream region (Fig.14). The velocity ratio is therefor <1.0 and according to [17] a smaller loss production occurs.

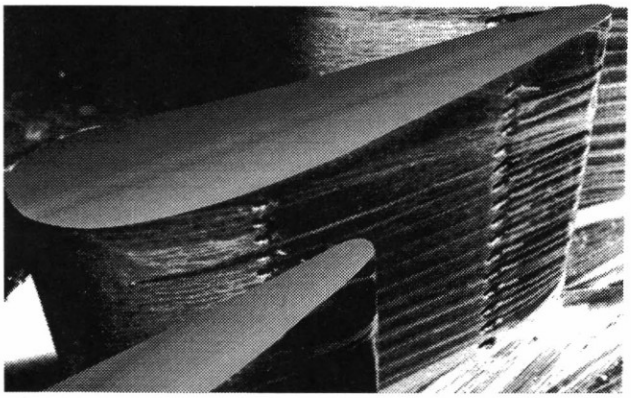

Fig. 14: Oilflow pattern for $M_1 = 0.85$ (row4)

Numerical simulations are very useful to support the studies in detail. A 3D-Navier-Stokes solver describes the stator flow with cooling air ejection out of row 4. The computational mesh exists in a multiblock version and consists as a whole of approximately 195000 cells. Cooling air ejection is realized through discrete cells of the mesh. The complex turbulent flow is described by applying the k-ε turbulence model in standard form. Important variables, like the Blowing ratio, the ejected mass flow and its direction is given and in agreement with the experiments. Further details about the flow solver can be found in [16]. The comparison between the oil flow experiments and the calculated streamlines on the suction side with varied Blowing ratios is shown in Fig.15. Above mentioned tendencies correspond well with the experiments. Thus, the extent of the region influenced by the secondary flow, the development of the cooling air jets and resultant uncooled areas can be analyzed without the unalterable slanted direction of sight in the experiments.

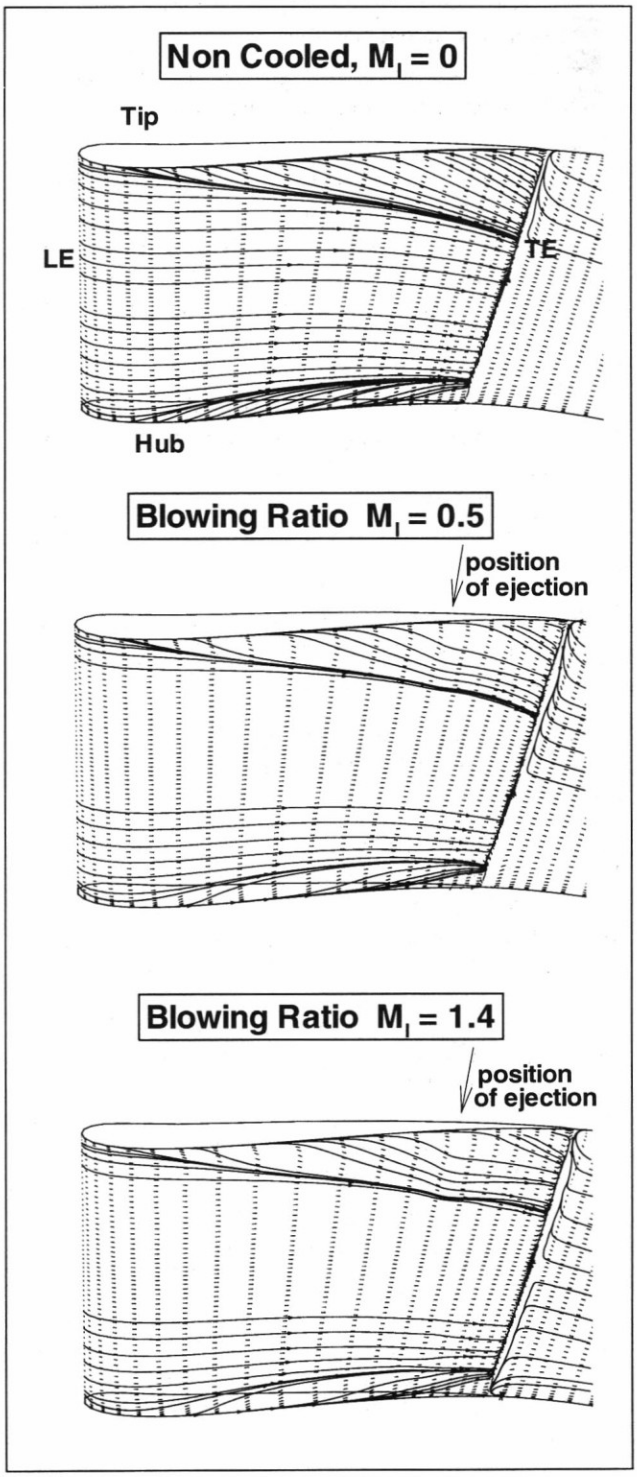

Fig. 15: Calculated streamlines on the suction side (cooling air ejection out of row 4)

Conclusions

- for zero ejection (M_1=0, cooling holes are present) the kinetic energy loss ζ_{kin} increases by nearly 1% compared to the smooth blade
- minimum mixing losses and kinetic energy loss production occur for $M_1 = 0.85$

- ζ_{kin} rise drastically for $M_1 > 0.85$ due to a stronger interaction with the mainflow
- the radial distribution of ζ_{kin} show strong differences at the tip, depending on the Blowing ratio

M_1=0.5

- the cooling air is deflected by the secondary flow and a faster mixing process occurs
  → the secondary flow region remained bad respectively non cooled
- the loss production due to acting shearing stresses is small

M_1=1.4

- the mass flux density in the secondary flow region is nearly three times higher compared to the mainstream region
  → disproportional strong cooling exists
- the loss production rises strongly since higher acting shearing stresses

- the applied visualisation and measuring technique are useful tools to study the mixing process of cooling air ejection

- numerical simulations of the stator flow with film cooling air ejection support the oil flow experiments.

Acknowledgements

The financial support of AG-Turbo, Germany to this project is acknowledged. The author wish to express her gratitude to Mr. Fischer, Mr. Karnatschke, Mr. Seelig and Mr. Voigt for their contribution to the executed measurements.

References

[1] Ajersch, P., Zhou, J., Ketler, S., Salcudean, M. and Gartshore, I. S.
"Multiple Jets in a Crossflow: Detailed Measurements and Numerical Simulations"
ASME 95-GT-9 (1995)

[2] Bons, J. P., MacArthur,C. D. and Rivir, R.
"The Effect of High Freestream Turbulence on Film Cooling Effectiveness"
ASME 94-GT-51 (1994)

[3] Burns, W.K. and Stollery, J.L.
"The Influence of Foreign Gas Injection and Slot Geometry on Film Cooling Effectiveness"
Int. J. of Heat and Mass Transfer, Vol. 12, (1981)

[4] Friedrichs, S., Hodson, H.P. and Dawes, W.N.
"Distribution of Film-Cooling Effectiveness on a Turbine Endwall Measured Using the Ammonia and Diazo Technique"
ASME 95-GT-1 (1995)

[5] Haller, B. S.
"The Effect of Film Cooling upon the Aerodynamic Performance of Transonic Turbine Blades"
Ph.D.-Thesis, University of Cambridge, Sept. 1980

[6] Haller, B.R. and Camus, J.-J.
"Aerodynamic loss penalty produced by film cooling transonic turbine blades"
J. of Engineering for GAS TURBINE and POWER, Vol. 106, No. 1, 1984, pp 188-205

[7] Hay, N., Lampard, D. and Benmansour, S.
"Effect of Crossflows on the Discharge Coefficient of Film Cooling Holes"
J. of Engineering for Power, Vol. 105, 1983

[8] Ito, S. , Eckert E.R.G. and Goldstein, R.J.
"Aerodynamic Loss in a Gas Turbune Stage with Film Cooling"
Transaction of the ASME, Vol. 102, 1980

[9] Jabbari, M. Y. and Goldstein, R. J.
"Adiabatic Wall Temperature and Heat Transfer Downstream of Injection through two Rows of Holes"
J. of Engineering for Power, Vol. 100, 1978

[10] Jubran, B. and Brown, A.
"Film Cooling From Two Rows of Holes Inclined in the Streamwise and Spanwise Direction"
ASME 84-GT-286 (19984)

[11] Kadotani, K. and Goldstein, R. J.
"On the Nature of Jets Entering a Turbulent Flow Part A: Jet-Mainstream Interaction"
J. of Engineering for Power, Vol. 101, 1979

[12] Kohli, A. and Bogard, D. G.
"Adiabatic Effectiveness, Thermal Fields and Velocity Fields with large Angle Injection"
ASME 95-GT-219 (1995)

[13] Köllen, O. and Koschel, W.
Effect of Film Cooling on the Aerodynamic Performance of a Turbine Cascade"
AGARD-CP-390 (1985)

[14] Kruse, H.
"Effects of Hole Geometry, Wall Curvature and Pressure Gradient on Film Cooling downstream of a Single Row"
AGARD-CP-390, 8-1/13 (1985)

[15] Langowsky, C. and Voigt, P.
"Film Cooling of an Annular Turbine Stator - Visualisation of Cooling Air Ejection and its Effect on the Aerodynamic Losses"
12th Symposium on Measuring Techniques, Prague, Septmber 1994

[16] Langowsky, C. and Vogel, D.T.
"The Influence of Film Cooling on the Secondary Flow in a Turbine Stator -
An Experimental and Numerical Investigation"
AIAA 95-3040 (1995)

[17] Lee, S. W. and Kim, Y. B.
"Flow Characteristics and Aerodynamic Losses of Film-Cooling Jets with Compound Angle Orientaion"
ASME 95-GT-38 (1995)

[18] Ligrani, P. M., Ciriello, S. and Bishop, D. T.
"Heat Transfer, Adiabatic Effectiveness and Injectant Distributions Downstream of a Single Row and Two Staggered Rows of Compound Angle Film-Cooling Holes"
Journal of Turbomachinery, Vol.114, 1992

[19] Marchal, Ph. and Sieverding, C. H.
"Secondary Flows within Turbomachinery Bladings"
AGARD-CP-214 (1977)

[20] Mehendale, A. B. and Han, J. C.
"Influence of High Mainstream Turbulence on Leading Edge Film Cooling Heat Transfer"
ASME 90-GT-9 (1990)

[21] Pietrzyk, J. R., Bogard, D. G. and Crawford, M. E.
"Hydrodynamic Measurements of Jets in Crossflow for Gas Turbine Film Cooling Application"
ASME 88-GT-174 (1988)

[22] Sen, B., Schmidt, D. L. and Bogard, D. G.
"Film Cooling with Compound Angle Holes: Heat Transfer"
ASME 94-GT-311

[23] Pedersen, D.R., Eckert, E.R.G. and Goldstein R.J.
"Film Cooling with Large Density Differences between the Mainstream and the Secondary Fluid Measured by the Heat-Mass Transfer Analogy"
Transaction of the ASME, Vol. 99, 1977

[24] Wang, H., Olson, S. J., Goldstein, R. J. and Eckert, E. R. G.
"Flow Visualisation in a Linear Turbine Cascade of high Performance Turbine Blades"
ASME 95-GT-7 (1995)

[25] Wilfert, G. and Fottner, L.
"The aerodynamic mixing effect of discrete cooling jets with mainstram flow on a highly loaded turbine blade"
ASME 94-GT-235 (1994)

[26] Yamamoto, A., Kaba, K. and Matsunuma, T.
"Measurement and Visualization of Tree-Dimensional Flows in a Linear Cascade"
ASME 95-GT-341 (1995)

[27] Yamamoto, A., Kondo, Y. and Murao, R.
"Cooling-Air Injection into Secondary Flow and Loss Fields Within a Linear Turbine Cascade"
ASME 90-GT-141 (1990)

[28] Yoshida, T., Minoda, M., Sakata, K., Nouse, H., Takahara, K. and Matsuki, M.
"Low- and High-Speed Cascade Tests of Air-Cooled Turbine Blades"
ASME 76-GT-40 (19970)